Measurement Science and Technology, Volume 12, Number 2, 2001, Pages 181-187

TIME-DIVISION-MULTIPLEXED INTERROGATION OF FIBRE BRAGG GRATING SENSORS USING LASER DIODES

A. Wilson, S.W. James & R.P. Tatam

Optical Sensors Group, Centre for Photonics and Optical Engineering,

School of Mechanical Engineering, Cranfield University, Cranfield,

Bedford, MK43 0AL, UK.

Tel 01234 754630

Fax 01234 750728

Email r.p.tatam@cranfield.ac.uk

Abstract

An intensity-based technique for the interrogation of fibre Bragg grating sensors is described. The technique utilises two longitudinal modes of a single, pulsed laser diode as a dual-wavelength source for grating illumination. Time-division-multiplexed addressing of sensor arrays in serial and tree topologies is also demonstrated.

1 *Introduction*

The fibre Bragg grating (FBG) has demonstrated its potential for use as a sensing element in a variety of optical fibre sensing applications [1,2]. FBG sensors offer a number of unique advantages over alternative optical fibre sensor types due to their localised nature and wavelength-encoded operation. In addition, it is possible to write many FBGs along a single fibre length, creating quasi-distributed FBG sensor arrays, which can be multiplexed in the wavelength, frequency, time and spatial domains.

A number of methods of determining the measurand induced Bragg wavelength shift from FBG sensors have been demonstrated. These include edge filters [3], volume holograms [4], tuneable filters [5], [6], matched receiving gratings [7], and interferometric techniques [8]. In general such demodulation systems employ a source with a broad spectral bandwidth, typically 10 nm -50 nm full width half maximum (FWHM), in conjunction with FBGs each with a narrow spectral width, typically 0.1 nm - 0.5 nm. Such schemes have been widely investigated, and a number of successful field and application trials have been reported.

An alternative approach that has received little attention since it was proposed by Morey[9] is the use of laser based interrogation of an array of FBGs fabricated with identical centre wavelengths. In this approach the FBG has a broad spectral bandwidth in comparison to the source. A potential advantage of using such a demodulation technique is the reduced complexity, and potentially reduced cost, associated with fabricating an array of identical FBGs.

2. Principle of operation

Laser interrogation of FBG sensors is, in essence, a passive filtering technique. Instead of employing a broadband optical source and a broad spectral filter to transduce measurand induced Bragg wavelength shifts into changes in intensity [3], the FBG itself is used as a spectral filter, with the measurand induced wavelength shift inducing a change in reflectivity at the laser wavelength.

The principle of the technique is illustrated in Fig.1. The FBG is simultaneously illuminated at two wavelengths. The wavelengths are chosen such that the Bragg centre wavelength, λ_B, lies mid-way between them. The FBG acts as a double edge filter, with opposite polarity filtering slopes for the two illuminating wavelengths. Measurand induced perturbations of the FBG result in a change in the intensities of the light reflected at the two wavelengths, the opposite polarity of the filtering slopes causing the magnitude of one component to increase while the other decreases. Processing the separately detected outputs using the following algorithm

$$S = \frac{I_{\lambda_1} - I_{\lambda_2}}{I_{\lambda_1} + I_{\lambda_2}} \qquad [1]$$

where $I_{1,2}$ are the intensities of the reflected components at wavelengths λ_1 and λ_2 respectively, results in an output that is proportional to the magnitude of the applied measurand. The output of this algorithm will be linear over a measurand range corresponding to the linear portions of the grating filtering edges. The algorithm also provides a self-referencing mechanism to compensate for source intensity fluctuations and down-lead losses; non-measurand induced intensity changes will be present on

both reflected components, causing the output of the algorithm to remain unchanged. Modulation of the output power of the laser sources allows an array of FBG sensor elements, fabricated at the same centre wavelength, to be addressed using time-division-multiplexed (TDM). A single pulse of the source produces a comb of reflected pulses, the separation of the reflected pulses in time being dependent upon the physical separation of the sensor elements. Each FBG element within the array is then identified by the time of flight of its reflected pulse

The illuminating wavelengths can be derived from two separate single longitudinal mode laser sources. The use of two separate sources requires careful control of the laser drive conditions to maintain a stable wavelength separation, and complicates the fibre coupling system. The preferred approach, adopted here, is to use a single source that operates simultaneously at two closely spaced wavelengths. The recently reported two-longitudinal-mode distributed Bragg reflector laser diode [10] would be an attractive candidate for this scheme. However, such a device is not currently commercially available. It has previously been demonstrated that laser diodes with Fabry-Perot cavities, operated with pulsed injection currents [11], or under the influence of feedback levels of as little as –60 dB [12], can exhibit spectra dominated by two longitudinal modes. Thus, by appropriate choice of operating conditions, low cost laser sources could be used as a dual-wavelength source. A discussion of the critical parameters for achieving this operating regime will be discussed in the following section.

2.1 Laser Characteristics

The source used was a Sharp laser diode (LT015MDO), operating at a wavelength of 830nm with an output power of 30 mW. The injection current supply and thermoelectric temperature controller had long term stabilities of ≤10 μA, and <0.005 °C respectively. The laser diode was mounted in a laser head equipped with a BIAS-T, which allowed external modulation of the injection current from 5MHz to 1 GHz. The laser was pre-biased to just below its injection current threshold, to eliminate turn-on delay effects that might modify the temporal profile of the output pulses. Square-wave modulation of the injection current was performed using a pulse generator with a 300 MHz bandwidth and 300ps rise/fall times. The injection current was pulsed at a frequency of 25MHz, with a pulse width of 6ns. Control of the laser bias current, modulation current and temperature, allowed the output of the laser to be tuned such that two longitudinal modes, separated by two cavity modes (~0.6nm), dominated the spectrum. Figures 2 and 3 show the dependence of the spectral profile of the laser output upon bias current and operating temperature. The power in the two modes can be equalised by appropriate choice of operating current and temperature. The spectral profile arises through hole-burning effects in the laser cavity [13]. Characterisation of the laser output indicated the observed spectrum to be stable over a number of hours and reproducible over a period of greater than one year. Investigation of other laser diodes of the same type showed that they also could be tuned to operate with similar spectral profiles [14].

A potential limitation to the performance is the wavelength shift associated with the pulsing of the laser (chirp) [15]. This chirp produces an apparent shift in the FBG

wavelength that is indistinguishable from a measurand induced shift. To assess the magnitude of this effect the chirp behaviour of the laser was measured using a path length imbalanced Michelson interferometer. The magnitude of the chirp was found to vary as a function of pulse duration, pulse frequency and the amplitude of the modulation current applied. However, under constant operating conditions the chirp was found to be highly reproducible. For the same conditions as used in the sensor experiments described in the next section the magnitude of the chirp was measured to be 1GHz. The effect of the chirp is to produce a constant offset in the value of the recovered measurand. For example, a 1GHz chirp produces an overestimate in the measured strain of 4$\mu\varepsilon$. The measurements can be compensated for the effects of chirp provided the characteristics of the laser are known.

2.2 Crosstalk

The use of a serial array of FBG sensors with the same centre wavelength results in crosstalk between sensors. A measurand induced change in the FBG centre wavelength causes a change in the reflected intensity and a concomitant change in the transmission of the FBG, and thus in the optical power incident upon subsequent FBG sensor elements in the array. The amount of light reflected by the FBG sensors located nearest to the source will affect the amount of the optical power reaching and being returned from gratings further from the source. The lower the peak reflectivity of the FBGs, the smaller the effect. The light reflected from the n^{th} FBG in a serial array of identical sensors is given by:

$$I_n = I_o R (1-R)^{2(n-1)} \quad (1)$$

Where I_o is the power coupled into the fibre and R is the FBG reflectivity.

For example, for peak FBG reflectivities of 0.1% the difference between the light returned from the tenth FBG in the array when all FBGs are in their quiescent state, that is reflecting 0.05% of the incident power, and when they all have zero reflectivity at the laser wavelength, is 0.9%. That corresponds to a crosstalk level of approximately 20dB. This is the worst case assuming that no account is taken of the variation of the power returned by the FBGs in the array. However, if we assume that the intensity from each sensor can be measured to 1% then the amount of power returned from each sensor can be compensated for the effect of previous FBGs in the array. For example, the intensity reflected from the tenth sensor will be measured to an accuracy of 3.1%. Thus the crosstalk is reduced to 3.1%*0.9% equivalent to 35.5dB. For an array of 25 sensors this increases to 29.2dB and for 100 sensors to 20.3dB.

Another source of crosstalk in a time-division multiplexed serial array of identical FBG sensors arises from multiple reflections between FBGs. This can lead to pulses arriving simultaneously at the detector having undergone a direct reflection from a sensor element and also having experienced a number of multiple reflection paths between FBGs. For low reflectivity FBGs only first order multiple reflections need to be considered. It can be shown that the number of multiple reflection routes, n_p, that have a significant effect on the crosstalk is [16]

$$n_p = \frac{(m-1)(m-2)}{2} \qquad (1)$$

For example, for ten FBGs there are 36 different paths for first-order reflections, contributing a crosstalk level of 44.4dB. This increases to 23.1dB for 100 sensors. In

this scheme, where the measurand changes the reflectivity of the sensors, the limiting noise factor is given by the resolution with which the intensity of each sensor can be measured and used to adjust the readings from subsequent sensors. For low reflectivity sensors the effect of changes in the reflectivity of the sensors on subsequent sensors in the array dominates the crosstalk for sensor numbers up to approximately 100. At this point the crosstalk due to multiple reflections becomes comparable.

3. Experiment

A schematic diagram of the experimental system used to interrogate a serial array of FBG sensors is shown in Figure 4. The end of the optical fibre was polished at an angle of 8° to reduce feedback effects, and the laser spectrum was observed to be unaffected by the insertion of a Faraday isolator. The FBGs were illuminated via a 3dB coupler, which also provided a return path for the reflected pulses from the FBG sensing elements to the detector. The two interrogation wavelengths returned with each reflected pulse were spatially separated using a monochromator, and detected on individual avalanche photodiodes (electrical bandwidth 100MHz). An 8-bit digital oscilloscope/PC combination was used to display the pulse trains and perform signal processing. Reflected components were averaged over 20 pulse returns to reduce the effects of mode partition noise. The FBGs were mounted on piezoelectrically controlled translation stages to enable the application of quasi-static extension, and thus strain. TDM of the sensor array was achieved by the incorporation of fibre delay lines, the return pulse signals from any particular sensor in the array being identified by their time of arrival at the detectors. The system was configured such that a portion of each pulse from the laser diode was delivered to the monochromator to act as a

reference to monitor the relative intensities in the two longitudinal modes. This could be used to normalise for relative intensity variations, or to act as part of a feedback circuit to adjust the laser's operating conditions to maintain equal powers. The reference pulses were temporally separated from the signal pulses by incorporation of fibre optic delay lines.

The optimum FBGs for this demodulation system would have a linear filtering edge, with bandwidth suited to the strain range likely to be encountered within a given application. Such FBG fibre edge filters [17] were unavailable for this work and two alternative FBG configurations were employed to demonstrate the technique. Two types of FBG sensor were used to evaluate using the technique.

Single sensor operation was demonstrated using a relatively broad FBG (FWHM ~0.6nm, reflectivity ~2.5%), the spectrum of which is shown in figure 5. The second sensor type consisted of two collocated narrow-band FBGs, written such that their half-maximum reflectivity wavelengths were separated by ~0.6nm, as illustrated in figure 6. The FBGs were fabricated with reflectivities of approximately 2.5 % and FWHM of approximately 0.1 nm, at centre wavelengths 836.2 nm and 837 nm respectively. This 'double' FBG has the same effective bandwidth as the broadband FBG but is significantly easier to reproduce. The serial array comprised of three similar FBGs of this type. FBGs were fabricated in hydrogen loaded Spectran FS SMC-AO780B fibre using a tuneable UV source in a configuration that allowed fine control of the spectral characteristics of the FBGs [18], necessary to match the FBGs to the laser diode's operating wavelengths.

The fibre delay lines were ~1m long, giving a pulse separation of ~10ns. The pulse repetition rate was limited by the bandwidth of the avalanche photodiodes (APD's). However characterisation of the source spectral profile showed it to be unchanged when pulsed at 50MHz and the use of APDs with larger bandwidths would allow sensor separation to be halved.

4. Results and Discussion

Figure 7 shows a plot of *S,* calculated using equation 1, against applied strain for single sensor interrogation. By fitting a straight line to the linear portion of the graph a measurement range of $\pm 180 \mu\varepsilon$ (micro-strain) with a resolution of $\pm 3.1 \mu\varepsilon$ (determined from the noise on individual data points) was obtained. Calibration of the curve extends the range to $\pm 300 \mu\varepsilon$, albeit with reduced sensitivity at the extremes.

Figure 8 is a plot of the results obtained from the multiplexed 'double' FBG sensor array. Here, FBG 2 was subject to effective compression, FBG 3 was subject to extension, while FBG 1 was not subject to strain. From the plot, a range of $\pm 50 \mu\varepsilon$ with a resolution of $\pm 3.4 \mu\varepsilon$ was obtained. The equivalent temperature sensor based on this technique, assuming a FBG temperature sensitivity of 5.73 pm/°C, would have a range of 35 °C, with a resolution of 0.3 °C.

As discussed in section 2.2, low reflectivity FBGs are suitable for use in the serial array sensor topology, allowing the number of FBGs addressed to be maximised, while reducing the crosstalk between sensor elements.

The use of a different sensor topology such as the reflective tree array removes the cross talk imposed constraints on FBG reflectivity, allowing the use of high reflectivity FBG sensors. In addition, the two narrow-band FBGs can be written with arbitrary wavelength spacing, chosen to match the spectral characteristics of the source, making it possible to use laser diodes with different spectral output characteristics as the interrogating source. The optical configuration employed to investigate the performance of the tree topology is shown in figure 9. Fibre delay lines were incorporated to separate the returned pulses by 10 ns as shown in figure 10. The experimental procedure adopted was the same as that previously discussed, producing the results shown in figure 11. The results show improved strain resolution, due to the reduced crosstalk in the tree configuration.

The sensitivity of the sensor output, S, is dependent upon the gradients of the FBG filtering edges. Maximum sensitivity will be obtained from a FBG with equal gradient filtering edges and a FWHM reflection band equal to the separation of the illuminating wavelengths. Unequal filtering edge gradients will result in a reduction of the sensitivity. The results presented in figures 8 and 10 show differences between the gradients of S obtained from FBG1 and FBG2. This is a result of differences in the spectral characteristics of the two FBGs. The use of a phase mask for FBG fabrication [19] would produce FBG sensing elements with near identical characteristics.

The length of the FBG filtering edge limited the measurement range, while mode partition noise and the 8bit digitisation limit the resolution. Extended range may be possible using FBGs with tailored FBG edges [17,20], while the resolution would be

improved by the use of 10-bit digitisation. A 2nm long filtering edge [17] would yield a measurement range of approximately 4000 με, which, when combined with 10 bit digitisation, would provide a resolution limit of approximately 4με. This is compatible with the requirements of a number of structural monitoring applications. Multi wavelength laser sources with larger wavelength separations suitable to allow interrogation of such FBGs have been reported. Hole burning effects in multi-mode laser diodes have previously been shown to allow operation at two wavelengths spaced by upto 3nm[21]. The use of a two-longitudinal-mode distributed Bragg reflector laser diode [10] as the illuminating source offers reduced mode partition noise and therefore improved sensor resolution. In addition, two lasers operating at suitably separated wavelengths may be employed, since, as illustrated by figure 9, it is possible to derive a reference pulse at each wavelength to compensate for differential changes in the output powers. The availability of laser diodes operating over a wide range of wavelengths offers the potential for multiplexing large sensor arrays using a combination of WDM and TDM.

It is informative to compare the signal to noise ratio (SNR) offered by the TDM technique presented here with that of a conventional WDM system based around the use of a broadband optical source and scanning optical filter. It can be shown that, a laser with an output power of 10 mW used in conjunction with a FBG of maximum reflectivity 1% (limited by the crosstalk considerations discussed previously) leads to a reflected signal level that is approximately an order of magnitude larger than that provided by a system employing a broadband source of 1 mW output power, with a 50nm FWHM, used in conjunction with a FBG of 100% reflectivity and 0.1 nm FWHM. The required electrical bandwidths of the two systems are 100 MHz for the

TDM system, and 1MHz for a typical WDM system. Since the SNR is inversely proportional to the square root of the bandwidth, the two systems offer comparable SNRs. Laser diodes with higher output powers are readily available, offering potentially improved SNR performance.

The scheme offers a number of advantages over other interrogation techniques. The laser diode source is inexpensive, with relatively high output power. In addition, the source is capable of high frequency modulation, making it ideal for use in TDM systems. Finally, since the FBG sensing elements have identical characteristics, the fabrication process for making large sensor arrays is greatly simplified.

5. Conclusion

An intensity-based, self-referenced technique for interrogation of in-fibre Bragg grating sensing elements using a pulsed laser diode source has been presented. Two different types of FBG have been used to evaluate the technique and a single sensor range of $\pm 180 \mu\varepsilon$ with resolution of $\pm 3.1 \mu\varepsilon$ has been achieved. Results demonstrating TDM addressing of a serial array of three FBG sensors have been presented and techniques to extend the range discussed.

A.Wilson would like to acknowledge an Engineering and Physical Sciences Research Council (U.K.) studentship.

6. References

1 P. Ferdinand, 'Applications of Bragg grating sensors in Europe', 1997 in 12th International Conference on Optical Fibre Sensors, **16**, OSA Technical Digest Series, (OSA, Washington, DC) pp 14-17.

2 Y.J. Rao 'In-fibre Bragg grating sensors' Meas.Sci.Technol. 1997, **8**, 355-375

3 Melle, S.M., Lui, K. & Measures, R.M. 'Practical fibre-optic Bragg grating strain gauge system', *Appl. Opt*., 1993, **32**, pp 3601-3609.

4 James, S.W., Dockney, M.L. & Tatam, R.P. 'Photorefractive volume holographic demodulation of in-fibre Bragg grating sensors', *IEEE Photon Technol.Lett*., 1996, **8**, pp 664-666.

5 Kersey, A.D., Berkoff, T.A. & Morey, W.W. 'Multiplexed fibre Bragg grating strain sensor system with a Fabry-Perot wavelength filter', *Opt. Lett*., 1993, **18**, pp 370-1372.

6 Xu, M.G., Geiger, H., Archambault, J.L-., Reekie, L. & Dakin, J.P. 'Novel interrogation system for fibre Bragg grating sensors using an acousto-optic tunable filter', *Elect. Lett*., 1993, **29**, (17), pp. 1510-1511.

7 Jackson, D.A., Lobo Ribeiro, A.B., Reekie, L. & Archambault, J.L-. 'Simple multiplexing scheme for a fibre-optic grating sensor network', *Opt. Lett*., 1993, **18**, (14), pp. 1192-1194

8 Kersey, A.D., Berkoff, T.A. & Morey, W.W. 'Fibre optic Bragg grating strain sensor with drift compensated high-resolution interferometric wavelength-shift detection', *Opt. Lett*., 1993, **18**, (1), pp.72-74.

9 Morey, W.W. “Distributed fibre grating sensors” in Proceedings of the 7th Optical Fiber Sensors Conference, The Institution of Radio and Electronics Engineers, Australia, pp285-288, 1990.

10 Iio, S., Suehiro, M., Hirata, T. & Hidaka, T.: ‘Two-longitudinal-mode laser diodes’, *IEEE Photon. Technol. Lett*., 1995, **7**, (9), pp. 959-961.

11 Lau, K.Y., Harder, C. and Yariv A. ‘Longitudinal mode spectrum of semiconductor lasers under high speed modulation’ *IEEE J.Quantum Elect.*, 1984, **QE-20**, pp70-79.

12 De Groot, P.J. ‘Range dependent optical feedback effects on the multimode spectrum of laser diodes’ *J. Mod.Opt*,. 1990, **37**, pp 1199-1214.

13 Yamamoto, Y., ed., *Coherence, Amplification and Quantum Effects in Semiconductor Lasers* (Wiley, New York, 1991).

14 A. Wilson, ‘Interrogation techniques for short gauge length optical fibre sensors’ PhD Thesis, Cranfield University 1998.

15 Sudbo, A.S. “Rate equation models and wavelength modulation in semiconductor diode lasers”, IEEE Journal of Quantum Electronics, 1987, QE-23, pp1127-1134,.

16 B. Culshaw “Distributed and multiplexed fibre optic sensing systems”, Proc.SPIE 1987 **132**, pp165-184

17 Liu Y., Zhang, L., Bennion, I., ‘Fabricating fibre edge filters with arbitrary spectral response based on tilted chirped grating structures’, Meas.Sci.Technol. 1998, **10**, pp 1-3

18 Dockney, M.L., James, S.W. & Tatam, R.P. ‘Fibre Bragg gratings fabricated using a wavelength tuneable laser source and a phase mask based interferometer’, *Meas. Sci. Technol*., 1996, **7**, (4), pp. 445-448

19 K.O. Hill B. Malo, F. Bilodeau, D.C. Johnson and J. Albert, 'Bragg gratings fabricated in monomode photosensitive optical fibre by UV exposure through a phase mask' Appl.Phys.Lett. **62**, pp. 1035-1037 (1993).

20 Kersey, A.D., Davis, M.A. and Tsai, T. 'Fibre optic Bragg grating strain sensor with direct reflectometric interrogation' in *Proceedings of the 11th Optical Fibre Sensors Conference*, (Sapporo, Japan, 1996), paper Th4-5, pp.634-637.

21 Ezbiri A. and Tatam R.P. 'Passive signal processing for a miniature Fabry-Perot interferometric sensor with a multimode laser diode source' Opt.Lett. **20**, pp1818-1820 (1995).

Figure captions

Fig. 1. Schematic illustrating dual-wavelength interrogation technique; (a) FBG unperturbed, intensity of reflected components equal, (b) FBG perturbed, Bragg centre wavelength shifts to λ_B', reflected components differentially filtered by FBG edges.

Fig. 2. Dependence of the spectral profile of the pulsed laser diode upon the bias current.

Fig. 3. Dependence of the spectral profile of the pulsed laser diode upon the operating temperature.

Fig. 3. Schematic of the experimental set-up for interrogation of an array of three FBG sensors using a serial topology. C, 3dB coupler; DL, delay line; L, divergent lens; APD, avalanche photodiode; DSO, digital storage oscilloscope; PC, computer; sig., return signal pulses.

Fig. 5. Fibre Bragg grating spectrum. The Bragg wavelength, and FWHM of the spectrum were tailored to the characteristics of the laser diode source.

Fig. 6. Spectrum returned from two co-located FBGs, which formed the "double grating" sensor. The FBGs were fabricated such that their half-maximum reflectivity wavelengths were separated by 0.6nm to match the separation of the longitudinal modes of the laser diode.

Fig. 7. Plot of S v applied strain for single sensor interrogation.

Sensor range ±180με, sensor resolution ±3.1με.

Fig. 8. Plot of S v applied strain for multiplexed sensor array in a serial topology.

Sensor range ±50με, sensor resolution ±3.4με.

Fig. 9. Schematic of experimental set-up for interrogation of array of three FBG sensors using a tree topology. C, 3dB coupler; DL, delay line; L, divergent lens; APD, avalanche photodiode; VC, variable splitting ratio directional coupler; DSO, digital storage oscilloscope; PC, computer; sig., return signal pulses.

Fig. 10. Digital Oscilloscope traces of the pulses returned from the reflective tree FBG sensor array.

Fig. 11. Plot of S v applied strain for multiplexed sensor array in a tree topology.

Sensor range ±50με, sensor resolution ±3.4με.

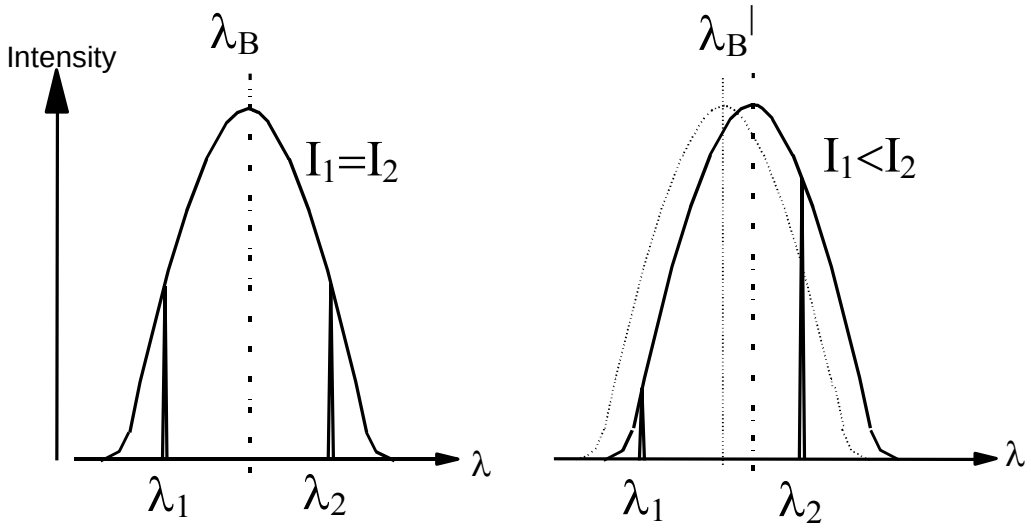
Intensity
λ_B
$I_1=I_2$
λ
λ_1
λ_2
λ_B'
$I_1<I_2$
λ
λ_1
λ_2

Figure 1.

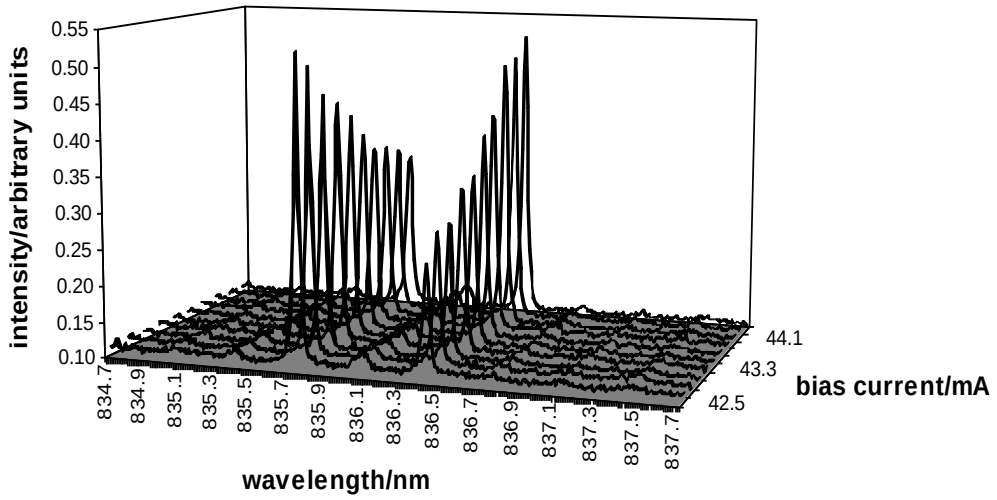
intensity/arbitrary units
0.55
0.50
0.45
0.40
0.35
0.30
0.25
0.20
0.15
0.10
834.7
834.9
835.1
835.3
835.5
835.7
835.9
836.1
836.3
836.5
836.7
836.9
837.1
837.3
837.5
837.7
wavelength/nm
42.5
43.3
44.1
bias current/mA

Figure 2

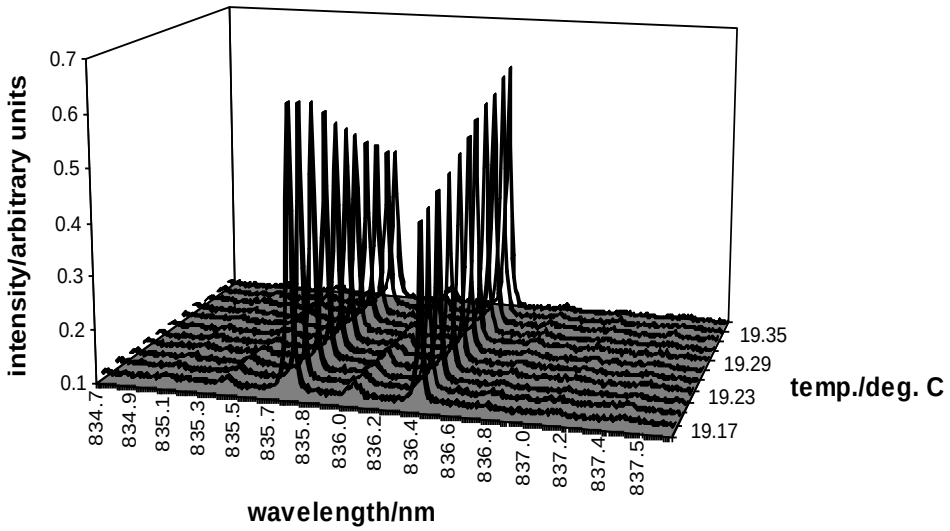
intensity/arbitrary units
0.7
0.6
0.5
0.4
0.3
0.2
0.1
834.7
834.9
835.1
835.3
835.5
835.7
835.8
836.0
836.2
836.4
836.6
836.8
837.0
837.2
837.4
837.5
wavelength/nm
19.35
19.29
19.23
19.17
temp./deg. C

figure 3

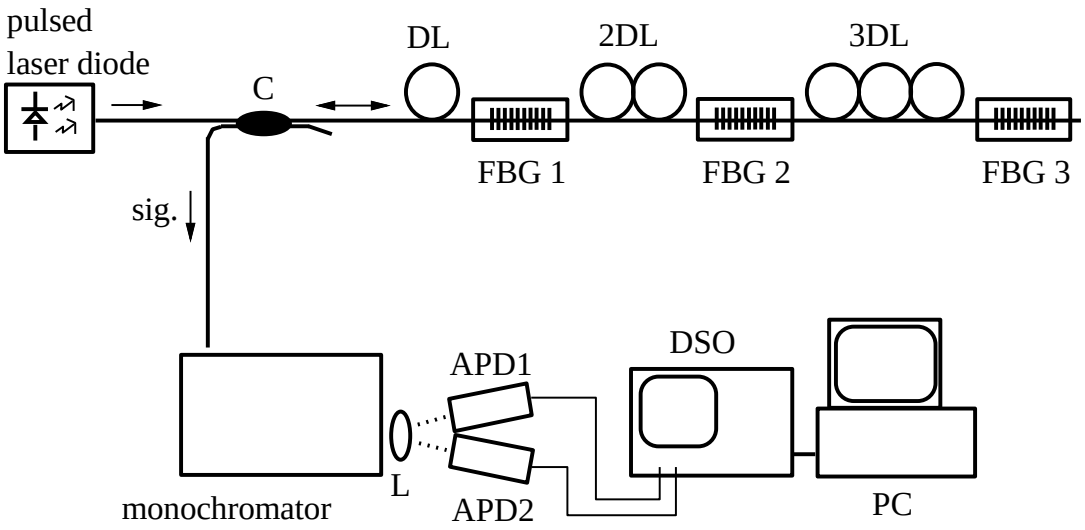
pulsed
laser diode
C
DL
2DL
3DL
FBG 1
FBG 2
FBG 3
sig.
APD1
DSO
L
monochromator
APD2
PC

Figure 4.

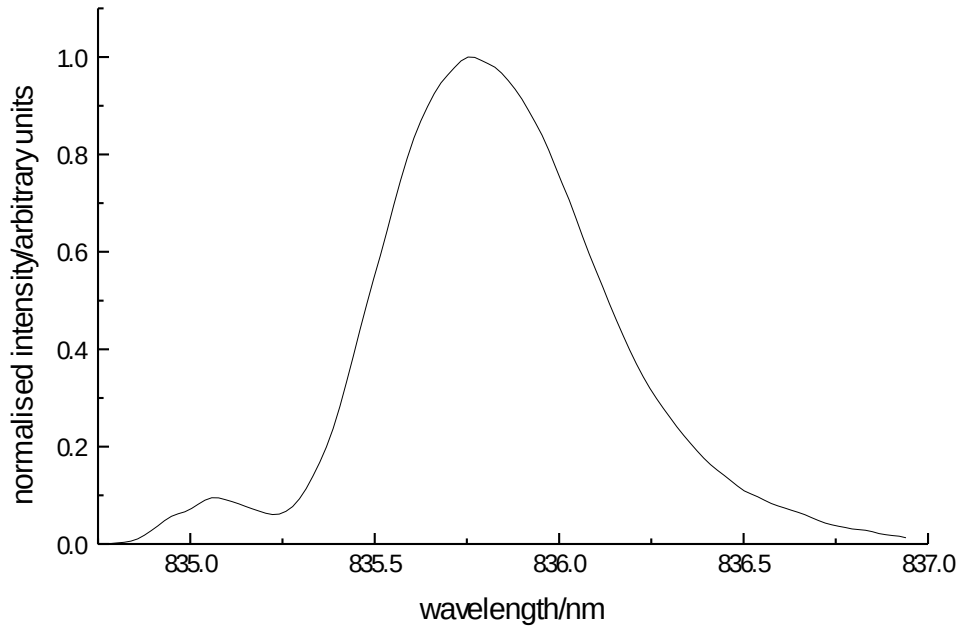
normalised intensity/arbitrary units
1.0
0.8
0.6
0.4
0.2
0.0
835.0
835.5
836.0
836.5
837.0
wavelength/nm

Figure 5

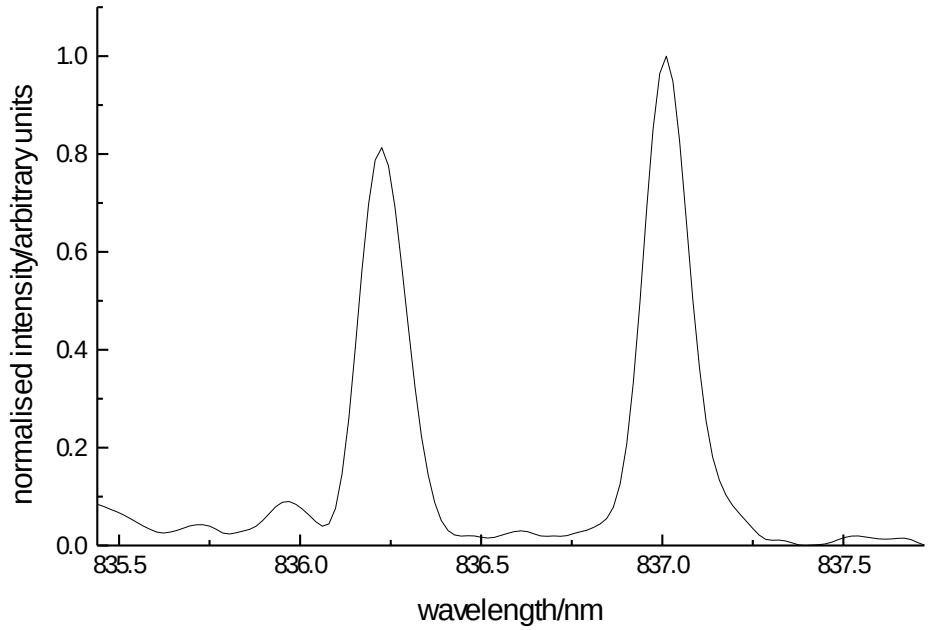
normalised intensity/arbitrary units
1.0
0.8
0.6
0.4
0.2
0.0
835.5
836.0
836.5
837.0
837.5
wavelength/nm

Figure 6

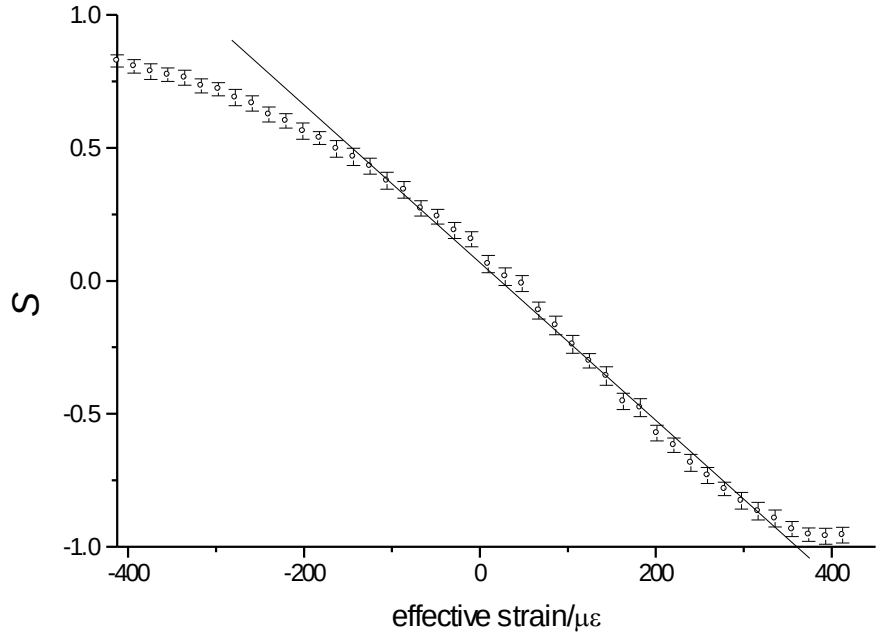

figure 7

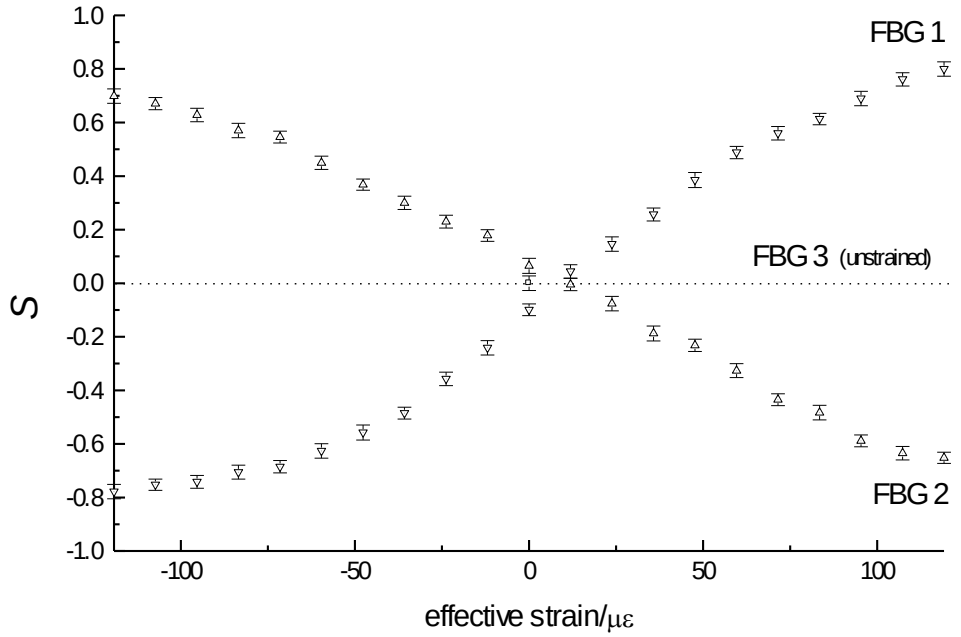
FBG 1
FBG 3 (unstrained)
FBG 2
S
effective strain/με
1.0
0.8
0.6
0.4
0.2
0.0
-0.2
-0.4
-0.6
-0.8
-1.0
-100
-50
0
50
100

figure 8.

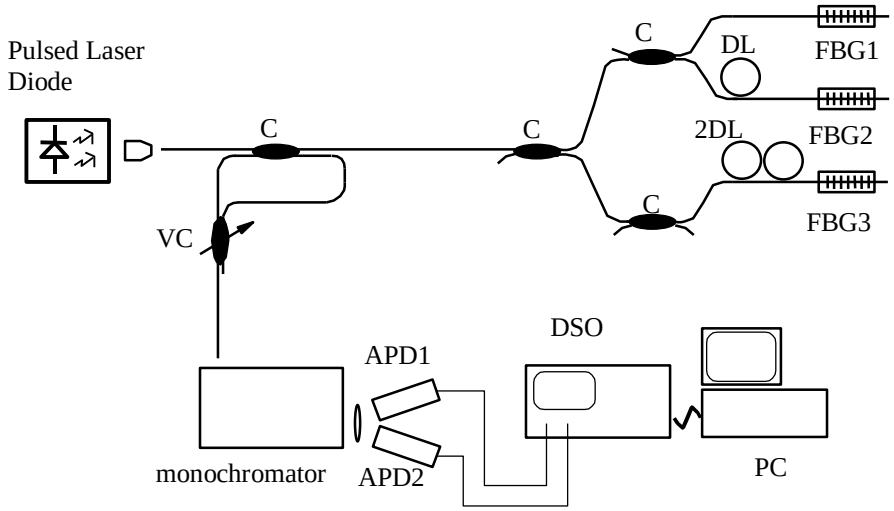
Pulsed Laser
Diode
C
C
C
DL
FBG1
2DL
FBG2
C
FBG3
VC
DSO
APD1
monochromator
APD2
PC

Figure 9

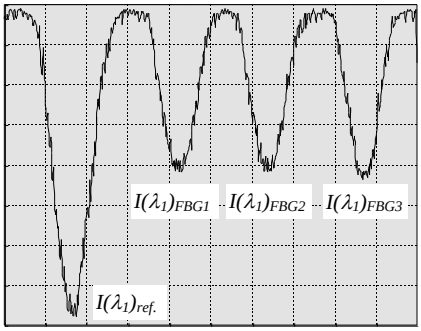

APD1

amplitude ; 5mV/div.
time-base ; 5nsec/div.

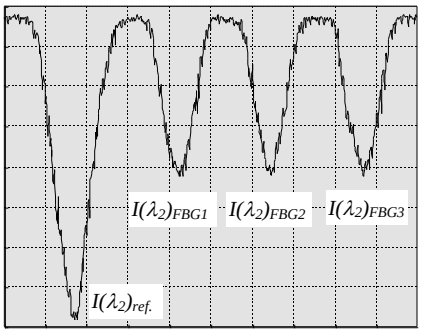

APD2

amplitude ; 5mV/div.
time-base ; 5nsec/div.

figure 10

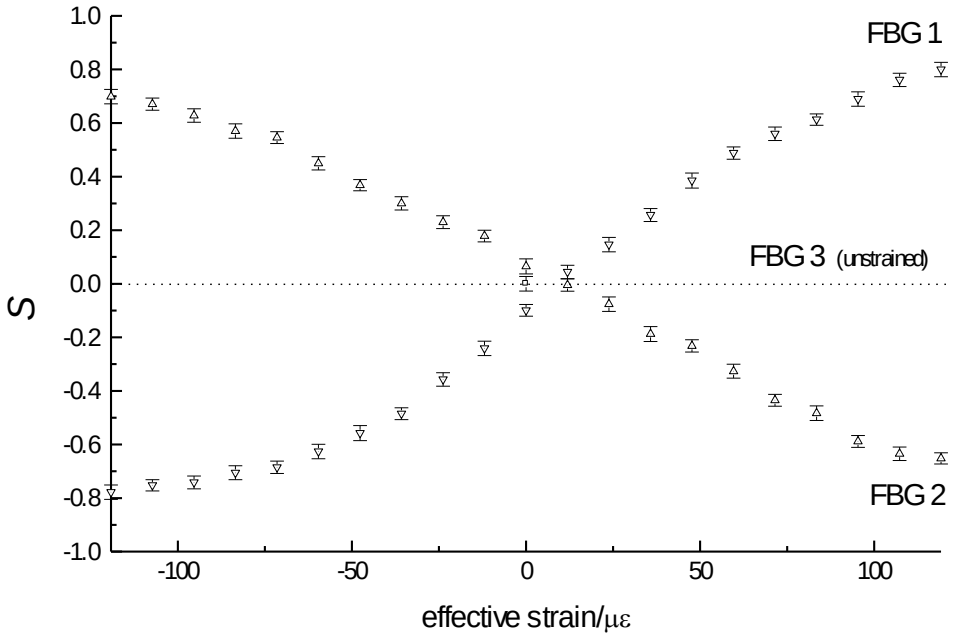
1.0
0.8
0.6
0.4
0.2
0.0
-0.2
-0.4
-0.6
-0.8
-1.0
S
-100
-50
0
50
100
effective strain/με
FBG 1
FBG 3 (unstrained)
FBG 2

figure 11